Available online at www.sciencedirect.com

ScienceDirect

Procedia Structural Integrity 2 (2016) 2598–2605

Structural Integrity Procedia

www.elsevier.com/locate/procedia

21st European Conference on Fracture, ECF21, 20-24 June 2016, Catania, Italy

Modeling of Brittle Crack Propagation/Arrest Behavior in Steel Plates

Kazuki Shibanuma[a]*, Fuminori Yanagimoto[a], Tetsuya Namegawa[b], Katsuyuki Suzuki[c], Shuji Aihara[a]

[a]*Dept. Systems Innovation, Graduate school of Engineering, the University of Tokyo, 7-3-1, Hongo, Bunkyo-ku, Tokyo, Japan*
[b] *Dept. Systems Innovation, Graduate school of Engineering, the University of Tokyo, 7-3-1, Hongo, Bunkyo-ku, Tokyo, Japan (presently Nippon Steel & Sumitomo Metal Corporation)*
[c]*Research into Artifacts, Center for Engineering, the University of Tokyo, 5-1-5, Kashiwanoha, Kashiwa-shi, Chiba, Japan*

Abstract

To prevent brittle cracks from causing fatal damage to steel structures, it is needed that steels have enough crack arrestability. However, the brittle crack propagation/arrest behavior has not been explained theoretically enough from the aspect of energy balance and especially the long crack problem has remained as an important unsolved issue for some decades. The authors propose a new model based on local fracture stress criterion to solve the long crack problem. The model considers crack closure effect by uncracked side ligaments formed due to relaxation of plastic constraint progressing with SIF increasing. A simultaneous equation composed of four equations, which formulate local fracture condition, strain hardening, yield point, and dynamic SIF considering side ligaments, is solved to simulate a crack propagation in the model. To validate the model, we compared model simulations with some experiments. Some of them were conducted under the long crack problem condition and obtained the result that they showed good agreements, even under the long crack problem condition. This implies the long crack problem can be explained from the aspect of side ligament development due to the relaxation of plastic constraint.

Peer-review under responsibility of the Scientific Committee of ECF21.

Keywords: "brittle crackl propagation;local fracture stress;ESSO tests;steel;crack arrest"

* Corresponding author. Tel.:+81-3-5841-6565.
E-mail address: shibanuma@struct.t.u-tokyo.ac.jp

Copyright © 2016 The Authors. Published by Elsevier B.V. This is an open access article under the CC BY-NC-ND license (http://creativecommons.org/licenses/by-nc-nd/4.0/).
Peer review under responsibility of the Scientific Committee of ECF21.
10.1016/j.prostr.2016.06.325

1. Introduction

As brittle fracture may give serious damage to the steel structures like container ships, the concept of "double integrity" has been as important as the prevention of crack initiation. A recent guideline on brittle crack arrest design, Nippon Kaiji Kyokai (2009) published, requires arrest toughness K_{ca} is larger than 6000 $N/mm^{3/2}$ for steel plates whose thickness is less than 80mm. K_{ca} is obtained from crack arrest length and applied stress and evaluated as an Arrhenius function of temperature. Although K_{ca} is usually measured by temperature gradient ESSO tests with the standard specimen whose width is 500mm, K_{ca} in duplex tests with the wide size specimen whose width is 2400mm has been reported to be much larger than one obtained in standard size ESSO tests at the same temperature as shown in Fig.1. This trend cannot be solved by classical linear fracture mechanics which the concept of K_{ca} is based on since it was first reported by Kanazawa et al.(1973) and called as "the long crack problem". Although it had been attempted to study the problem based on energy balance, the fundamental concept to study dynamic crack, there were not any explanation which successfully gets the consensus among the researchers. Contrary to them, Machida et al. (1995) and Aihara et al.(1996) proposed a numerical model for brittle crack propagation and arrest behavior based on local fracture criterion considering the shape of crack front and the formation of side ligaments. The result of the model showed the good agreement with experiments in the limited specimen sizes, but did not explain the long crack problem. After that, Aihara et al. (2008) reported the deviation of K_{ca} from estimated curves of standard tests was observed in the extremely high applied stress conditions. They proposed the effect of those stress conditions on K_{ca} is equivalent to one observed in the long crack problem and relaxation of plastic constraint, which is the loss of plane strain at the crack front, was considered in their model. But, this model needed arbitrary parameters which did not have physical meanings. Based on above studies, a new model is presented to explain brittle crack propagation/arrest behavior including the long crack problem without any parameters which cannot be explained physically.

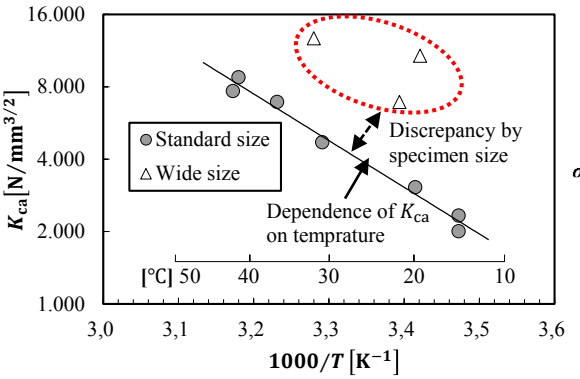

Fig. 1 Dependence of crack arrest toughness on temperature

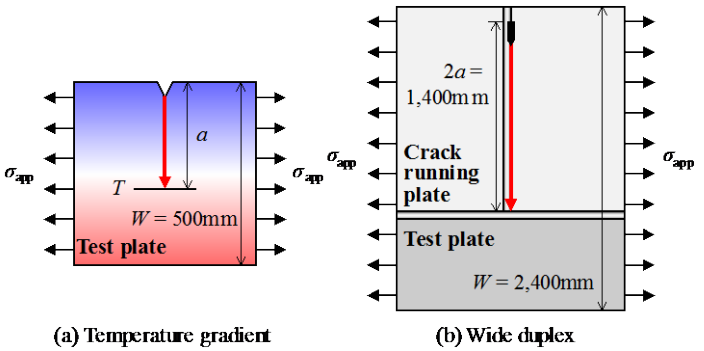

Fig.2 Type of brittle crack arrest tests

Nomenclature

d_{sl}	depth of uncracked sideligament
E_t	tangent modulus
K_d	dynamic stress intensity factor
K_p	stress intensity factor by a pair of point forces
K_{sl}	crack closure effect of uncracked side ligament as an expression of stress intensity factor
K_σ	stress intensity factor by remote tensile stress in infinite plate
L	length of plate
t	thickness of plate
W	width of plate
$\dot{\varepsilon}_e$	equivalent strain rate
ε_e	equivalent strain
ε_{zz}	plastic strain in the direction of thickness
σ_{app}	applied stress

σ_e	equivalent stress
σ_Y	yield stress
σ_{yy}	tensile stress

2. Model Formulation

2.1. Overview of the Model

A fundamental concept of a proposed model in our study is shown in Fig.3, whose detail contents are found in Shibanuma et al. (2016). We adopted three assumptions to construct the model formulation. The first assumption (1) is that a shape of crack front is assumed to be right angle to the direction of crack propagation, which is based on observations on fracture surface of past ESSO tests in Aihara et al. (2012). The second assumption (2) is that a cracked side ligament is considered as a part of crack and influences the stress intensity factor (SIF). It has been said that side ligament decreases the crack driving force as long as it is fractured in the ductile manners by previous studies, such as Ogura (1961) and Priest (1998). The last assumption (3) is that the formulation of the crack propagation is only evaluated at the crack front in the mid-thickness, which satisfies plane strain condition. This is much effective assumption to simplify the formulation and reasonable enough to simulate the crack behavior because the maximum crack length of cleavage fracture is generally obtained in the mid-thickness of the plates. Based on local fracture stress criterion, the crack continues to propagate as long as the local stress at the crack front $\sigma_{yy}[r_c, 0]$ is equal to the local fracture stress σ_f, which is regarded as a material characteristic value independent on crack velocity and temperature.

Based on the assumptions, the proposed model is composed of 4 equations to solve (a) fracture condition, (b) strain hardening, (c) yield point, and (d) dynamic SIF. The calculation proceeds by solving the equations simultaneously and the crack is regarded as to be arrested when the simultaneous equation cannot be solved or the uncracked side ligaments grow to reach the all the thickness. The detail formulations of four equations will be explained below.

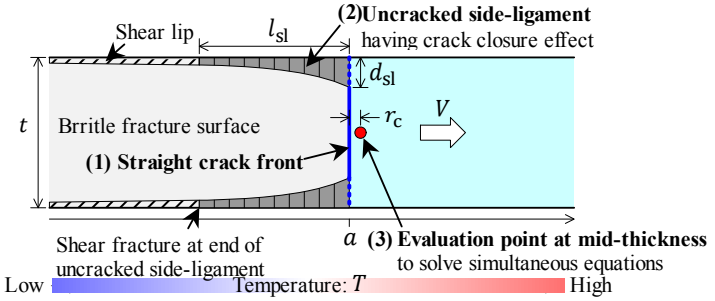

Fig.3 A schematic of the proposed model

2.2. Fracture condition

Fig.4 shows a schematic of brittle crack propagation in steel plates. The average tensile stress within a process zone have to be equal to fracture stress for the dynamic crack to continue to propagate as expressed

$$\sigma_f = \sigma_{yy}[r_c, 0] \tag{1}$$

The value of σ_f is a material constant value and r_c, which is the length of the process zone, is 0.3mm in this study considering the past studies such as Aihara et al. (2013). The value of σ_f is identified by using one experimental result.

Because there is no asymptotic solution of stress field in the vicinity of dynamic crack tips in elasto-plastic solids, the local stress at r_c is evaluated by combining the asymptotic solution for an elastic linear strain hardening materials, which was proposed by Machida et al. (1995). This combined equation is

$$\sigma_f = \sigma_{yy}[r_c, 0] = \sigma_Y \left\{ \frac{1-\nu^2}{r_c I_n} \left(\frac{K_d}{\sigma_Y} \right)^2 \right\}^{-s} \Sigma_{ij}[\theta, V] \tag{2}$$

Here, $\theta = 0$ and $\Sigma_{ij}[0, V] = 4$ for plane strain condition when V is lower than a half of the elastic Rayleigh wave

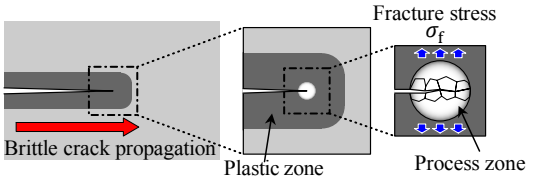

Fig.4 Local stress criterion for brittle crack propagation in steel

velocity. s, the stress singularity in a linear strain hardening solid, is expressed by $\alpha\ (=E_t/E)$ and $\beta\ (=V/V_s)$ as

$$s[\alpha,\beta]=s_0\left[\frac{\alpha-(\beta/0.57)^2}{1-(\beta/0.57)^2}\right] \tag{3}$$

The s derived from Eq.5 by Amazigo and Hutchinson (1977) are shown in Fig.5 made by Machida et al. (1995).

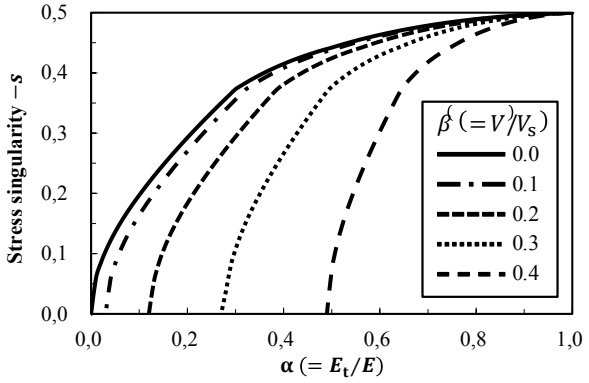

Fig. 5 Dependence of stress singularity on tangent modulus and crack velocity (Machida et al. (1995))

2.3. Strain hardening

Assuming the power law hardening solid, tangent modulus, E_t, is written in below equation.

$$E_t=\frac{d\sigma_e}{d\varepsilon_e}=nE\left(\frac{\sigma_e}{\sigma_Y}\right)^{-\left(\frac{1}{n}-1\right)} \tag{4}$$

Strain hardening exponent $n=0.2$ in this study. σ_e can be written as

$$\sigma_e[r,\theta]=\sigma_Y\left\{\frac{1-\nu^2}{rI_n}\left(\frac{K_d}{\sigma_Y}\right)^2\right\}^{-s}\Sigma_e[\theta,V] \tag{5}$$

In case of $\theta=0$, $\Sigma_e[0,V]$ is constant and set to 1.Therefore, a next equation is established.

$$E_t=nE\left[\left\{\frac{1-\nu^2}{r_cI_n}\left(\frac{K_d}{\sigma_Y}\right)^2\right\}^{-s[\alpha,\beta]}\Sigma_e[0,V]\right]^{-\left(\frac{1}{n}-1\right)} \tag{6}$$

2.4. Yield point

Yield point strongly depends on strain rate and temperature as widely known and can be written as

$$\sigma_Y=\sigma_{Y0}\exp\left\{(497.5-68.90\ln\sigma_{Y0})\left(\frac{1}{T}\frac{28.32}{18.42-\ln\dot{\varepsilon}_e}-\frac{1}{293}\right)\right\} \tag{7}$$

Eq.7 was reported by Gotoh et al. (1992) and Toyosada et al. (1994)

Using Eq.4, Eq.5, and Eq.6, strain rate at the process zone can be obtained from

$$\dot{\varepsilon}_e=\frac{\dot{\sigma}_e}{E_t}=-\frac{\sigma_Y}{E_t}\frac{Vs}{r_c}\left\{\frac{1-\nu^2}{r_cI_n}\left(\frac{K_d}{\sigma_Y}\right)^2\right\}^{-s}\Sigma_e[0,V] \tag{8}$$

2.5. Dynamic stress intensity factor considering uncracked side ligaments

Usually, the dynamic SIF is expressed as

$$K_{\mathrm{d}} = f_K[V]K \tag{9}$$

However, because, as mentioned, uncrack side ligaments are formed near the surfaces behind the propagating brittle crack front in steel plates and have the effect to decrease crack driving forces, this closure effect has to be considered to calculate the dynamic SIF as Eq.10.

$$K_{\mathrm{d}} = f_K[V](K_\sigma - K_{\mathrm{sl}}) \tag{10}$$

The depth of side ligaments is determined by the size of plastic zone at the crack tip, which is enlarged by the relaxation of plastic constraint as proposed by Aihara et al. (2013). Therefore, we considered this relaxation to formulate the brittle crack propagation/arrest behaviour to represent actual behaviours in our model. In this model, by assuming that the ligaments are elastic perfectly plastic solids and the closure effect is modelled by equivalent crack closure stress, the effect is regarded as equal to the yield stress of ligaments. According to Tada et al. (2000) considering a pair of point forces P,in a semi infinite crack in a 3D infinite body like Fig.7, K_{sl} is expressed as integration of SIF by P over the uncracked side ligament area, Ω_{sl} as Eq.11, which is shown in Fig.7 schematically.

$$K_{\mathrm{sl}} = \int_{\Omega_{\mathrm{sl}}} K_{\mathrm{p}}[x, z, \sigma_{\mathrm{Y}}\mathrm{d}\Omega] = \int_{\Omega_{\mathrm{sl}}} \frac{\sqrt{2}\sigma_{\mathrm{Y}}}{(\pi|x|)^{3/2}\cdot\{1+(z/x)^2\}}\mathrm{d}\Omega \tag{11}$$

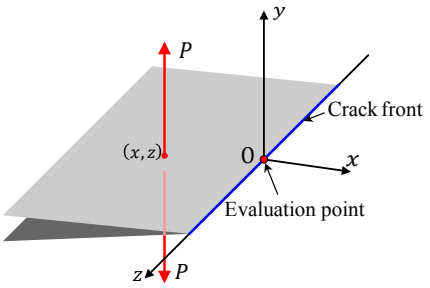

Fig. 6 Pair of point forces acting on a crack faces

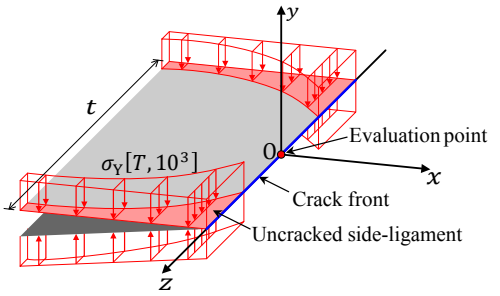

Fig.7 Crack closure stress on fracture surface t by side-ligament

As above, the depth of ligaments, being the surface zone where brittle fracture cannot occur due to decreasing stress triaxiality, is proportional to the size of a plastic region, r_{p}, according to Weiss and Senguputa (1976). We assumed

$$d_{\mathrm{sl}} = k_{\mathrm{sl}} r_{\mathrm{pd}} \tag{12}$$

$k_{\mathrm{sl}} = 2$ referring Weiss and Sengupta, (1976). r_{pd}, which is r_{p} in dynamic case, is approximated as

$$r_{\mathrm{pd}} = r_{\mathrm{p}}[K_\sigma] f_r[V] = \frac{f_r[V]}{6\pi}\left(\frac{K_\sigma}{\sigma_{\mathrm{Y}}}\right)^2 \tag{13}$$

To determine $f_r[V]$, which is hard to derive from simple theoretical ways, a series of FE analyses in Abaqus 6.14 (Dassault System (2014)) for a dynamic crack was conducted by using nodal force release technique to evaluate ε_{zz}.

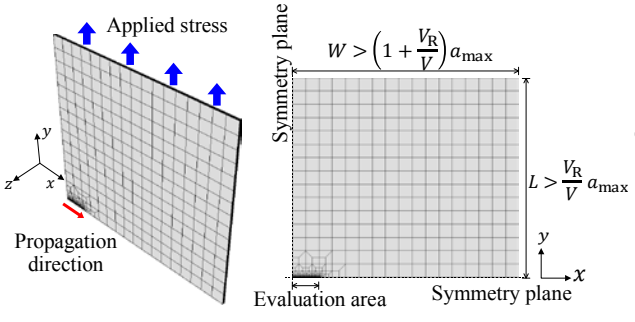

(a) Whole model (3D view) (b) Whole model (*xy* plane view)

Fig.8 Finite element mesh for dynamic crack propagation

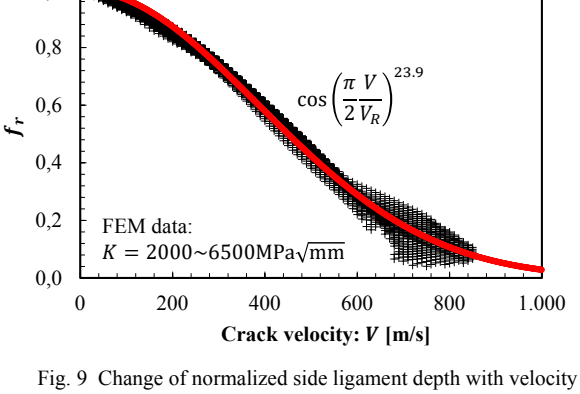

Fig. 9 Change of normalized side ligament depth with velocity

The analyses were done about various crack velocity with a 3D FE model shown in Fig.9 whose size is large enough for the reflected elastic wave not to influence the crack behavior. From these analyses, the value of ε_{zz} is obtained at the distance from the plate surface for each crack velocity. The distance corresponds to r_{p} in the quasi-static case and the ratio of the distance for each V to one of the quasi-static case were obtained as Fig.10 and Eq.15.

$$f_r = \left[\cos\left(\frac{\pi}{2}\frac{V}{V_{\mathrm{R}}}\right)\right]^{23.9} \tag{14}$$

The side ligament is considered as to be broken in ductile manners when the strain at the end of the ligament reaches critical strain, which is set to 0.1 in the present model.

As the result, the present model is calculated by solving simultaneous equations composed of Eq.2, Eq.6, Eq.8, and Eq.10 at each time step and the crack is regarded as being arrested when the equations cannot be solved.

3. Model validation

3.1. Crack arrest tests

To validate the present model temperature gradient ESSO tests using YP36 grade standard width specimen were implemented and duplex tests with wide width specimen in the condition of the long crack problem by Sugimoto et al. (2012) were referred The mechanical properties and dimensions of specimen are in Table 1 and the test results of YP36 and YP45 are shown in Table 2. Although K_{ca} at both temperature in the YP45 duplex tests is lower than SIF when a crack enters the test plate, the crack was arrested after propagating for some length in the test plate. This indicates cracks were arrested even in case of SIF $> K_{\mathrm{ca}}$. The fractions of the experiments are also shown in Fig.10.

Table 1 Mechanical properties and specimen dimensions of the used steels

YP36

Yield stress:σ_{Y0} [MPa]	Thickness [mm]	vE (-40°C) [J]	Plate width [mm]
368	30	354	500

YP45

Yield stress:σ_{Y0} [MPa]	Thickness [mm]	vE (-40°C) [J]	Width for wide duplex test [mm]	
			Crack ranning plate	Test plate
454	75	280	1,600	800

Table 2 Experimental conditions and results

YP36

Test type	Arrested crack length [mm]	Arrestted temperature [°C]	Applied stress [MPa]	Temperature	
				Top of plate T_0 [°C]	Gradient $\mathrm{d}T/\mathrm{d}x$ [°C/mm]
Temperature gradient	335.3	-18.6	93	-120.7	0.30
	257.2	-7.5	162	-84.7	0.30
	297.5	0.4	187	-98.1	0.33
	325.5	13	300	-85.9	0.31
	313.7	1.6	310	-92.0	0.30

YP45

Test Type	Applied stress [MPa]	Temperature [°C]	Arrest Toughness [N/mm $^{3/2}$]	Arrestted crack length [mm]
Duplex	257	-11	7000	1650
	257	-18	6100	1900

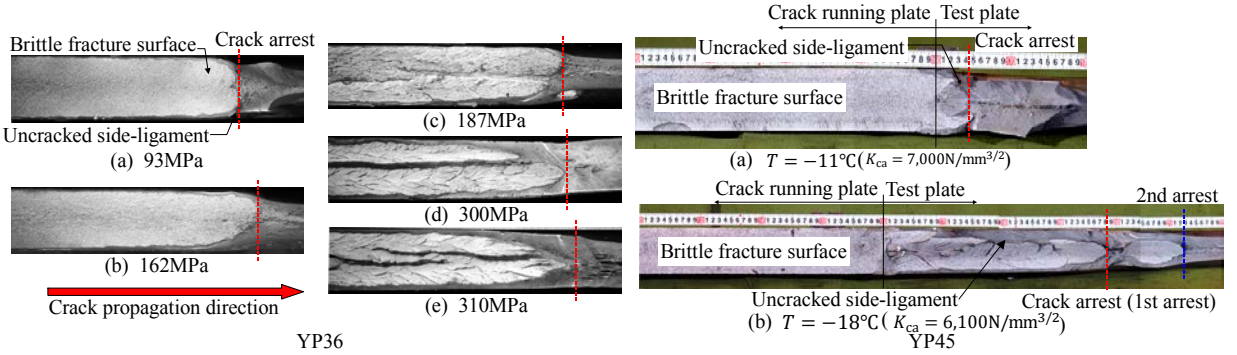

Fig.10 Fracture surface of YP36 and YP45 tests

3.2. Model simulation

Arrest toughness of YP36 steel was simulated by the model. The fracture stress was identified as 4370MPa so as to bring a simulation result in the condition that applied stress is 187MPa in line with the experimental result. All simulations on YP36 were done using this value of fracture stress. The prediction results by the model simulations in Fig.11 as Arrhenius plot show a good agreement with experimental data even on the deviation from Arrhenius equation under excessively high applied stress, which is assumed to be equivalent conditions to the long crack problem. Fig.12 shows predicted side ligament formation in the model simulations, which is much similar to the actual formation of side ligaments in above experiment.

Next, the model simulations of YP45 wide duplex tests were conducted to study crack behaviors in the long crack condition. Fracture stress of the steel was identified as 5295MPa by preliminary temperature gradient standard width tests as shown in Fig.13 in the same way as the YP36 steel. One of the crack running plate is set to 3707MPa, which is low enough not to cause of uncracked side ligament formation.

In the simulations using the above value as fracture stress, cracks were successfully arrested in both experimental conditions. The arrested crack lengths in the simulations are 1698mm in (a) and 1881mm in (b) respectively, which mostly agreed with the experimental results shown in Table 2. Additionally, in the simulations, the formation of side ligaments began just after a crack enter the test plate and rapidly developed during propagating in the plates as in Fig.14. According to Fig.10, same behavior of uncracked side ligament formation were observed in the actual tests.

Although according to conventional theoretical discussion based on linear fracture mechanics, cracks cannot be arrested as in the excessively high applied stress tests in YP36 temperature gradient tests and wide width tests in YP45 duplex tests, which in the long crack problem condition, because SIF is larger than K_{ca} estimated from Arrhenius

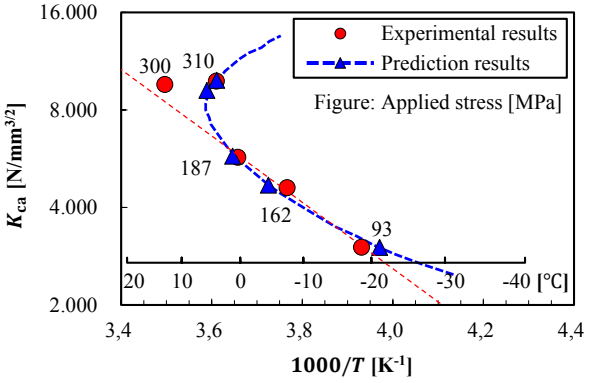

Fig. 11 Prediction results of dependence of arrest toughness on temperature for the YP36 steel by the temperature gradient tests

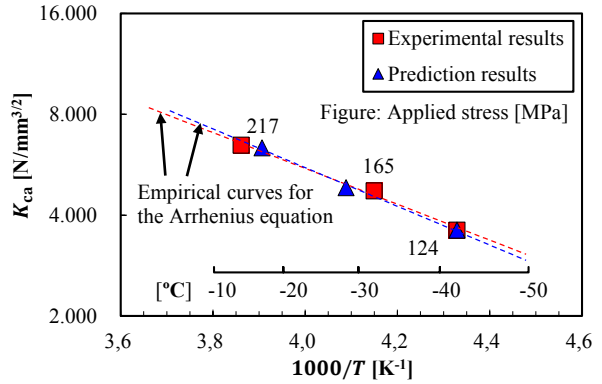

Fig. 13 Simulation results of dependence of arrest toughness on temperature for the YP45 steel by the temperature gradient tests

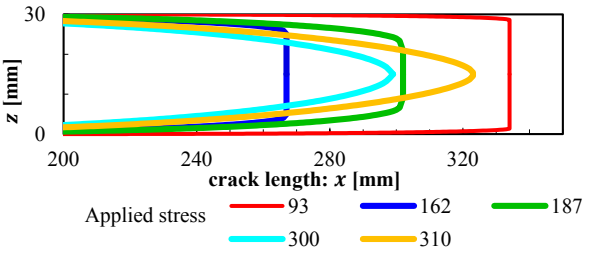

Fig.12 Simulated formation of side ligament for the YP36 tests

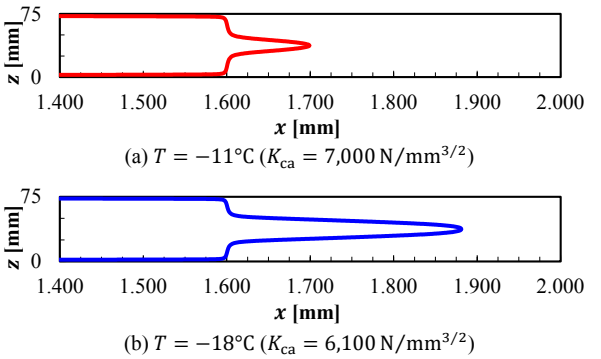

Fig.14 Simulated formulation of side ligaments in YP45 duplex tests

equation, the actual cracks were arrested in the tests, which were implied by the proposed model simulation that they can be explained from the aspect of development of uncracked side ligaments due to relaxation of plastic constraint.

4. Conclusion

The authors proposed a new model to simulate brittle crack propagation/arrest behavior in steel plates. The present model is able to predict crack arrestability quantitatively and evaluate circumstantial mechanisms on the behavior. Additionally, as discussed in last section, the model simulation show the good agreement even with the tests in the long crack problem condition, which implies the problem can be due to growth of side ligament with relaxation of plastic constraint incorporated in the model. It is expected that the model could contribute to devising the more reasonable crack arrest designs for steel structures.

Acknowledgements

Part of this study was supported by Nippon Kaiji Kyokai (classNK) and JSPS KAKENHI Grant Number 15H06661.

References

Achenbach, J.D., Kanninen, M.F., Popelar, C.H., 1981. Crack-tip fields for fast crack fracture of an elastic-plastic materials, Journal of the Mechanics and Physics of Solids 29, 211-225

Aihara S, Machida S, Yoshinari H, Mabuchi H, 1996. Fracture mechanical modeling of brittle fracture propagation and arrest of steel (2) - Application to temperature-gradient type test, Bulletin of The Society of Naval Architects of Japan 178, 545-554

Aihara S, Machida S, Yoshinari H, Tsuchida Y, 1996. Fracture mechanical modeling of brittle fracture propagation and arrest of steel (3) - Application to duplex type test, Bulletin of The Society of Naval Architects of Japan 179, 389-398

Aihara S, Shibanuma K, Watabe Y, 2013. Development of numerical model for brittle crack propagation/arrest behaviors. Journal of the Japan Society of Naval Architects and Ocean Engineers 16, 109-120

Amazigo, J.C., Hutchinson, J.W., 1971. Crack-tip, fields in steady-growth with linear strain hardening, Journal of the Mechanics and Physics of Solids 25, 81-97

Dassault Systems, 2014. SIMULA Abaqus Analysis User's Manual Version 6.14

Gotoh K., Toyosada, M., 1994. A simple estimating method of constitutive equation for structural steel as a function of strain rate and temperature, Journal of the Society of Naval Architects of Japan 176, 501-507

Hutchinson, J.W., 1968. Singular behavior at the end of a tensile crack in a hardening material, Journal of Mechanics and Physics of Solids 16, 13-31

Kanazawa T, Machida S, Yajima H, Aoki M, 1973. Study on brittle crack arrester: Consideration on the arrest of very long crack. Selected Papers from the Journal of the Society of Naval Architects of Japan 11, 135-147.

Machida S, Yoshinari H, Yasuda M, Aihara S, Mabuchi H, 1995. Fracture mechanical modeling of brittle fracture propagation and arrest of steel (1) - A fundamental model, Bulletin of The Society of Naval Architects of Japan 177, 243-257

Nippon Kaiji Kyokai, 2009. Guidelines on brittle crack arrest design

Ogura, N, 1961. A study on the Ductile Arrest of Brittle Cracks, Journal of Zosen Kiokai 110, 443-453

Priest, A.H., 1998. An energy balance in crack propagation and arrest, Engineering Fracture Mechanics 61, 231-251

Shibanuma, K., Yanagimoto, F., Namegawa, T., Suzuki, K., Aihara, S., 2016. Brittle crack propagation/arrest behavior in steel plate –Part I: Model formulation, Engineering Fracture Mechanics accpeted

Shibanuma, K., Yanagimoto, F., Namegawa, T., Suzuki, K., Aihara, S., 2016. Brittle crack propagation/arrest behavior in steel plate –Part II: Validation and discussion, Engineering Fracture Mechanics accepted

Sugimoto,K., Yajima, H., Aihara, H., Yoshinari, H., Hirota, K., Toyoda, M., Kiyose, T., Noue, T., Handa, T., Kawabata, T.,Tani, T., Usami, A., 2012. Thickness effect on the brittle crack arrest toughness value K_{ca}-Brittle Crack Arrest Design for Large Container Ships-6-, Proc. 22th Int. Offshore and Polar Eng. Conf., 4, 44-51

Toyosada, M., Gotoh K, 1992. The estimating method of critical CTOD and J integral at arbitrary crosshead speed, Journal of the Society of Naval Architects of Japan 172, 663-674

Tada, H., Paris, P.C., Irwin G.R., 2000. The stress analysis of cracks handbook, ASME Press

Weiss, V., Sengupta, M., 1976. Ductility, fracture resistance, and R-curves, ASTM Special Technical Publication, 194-207